bolic stroke [17]. This pathological process should be considered when we develop new therapeutic approaches for ischemic stroke.

Vascular endothelial growth factor (VEGF) is a unique growth factor for endothelial cells in the process of vasculogenesis and angiogenesis [3,19]. VEGF contributes to endothelial cell proliferation, vascular permeability, anti-apoptosis, and gene expression in endothelial cells. It has been demonstrated that VEGF is expressed by neurons, astrocytes, macrophages, and vascular cells in the ischemic brain [1,15,18]. Although there is no doubt that the endogenous VEGF expressed by these cells modifies the pathophysiological status, it is difficult to discern whether the effect of VEGF is favorable or unfavorable because of the multifunctions of VEGF. Angiogenesis by endothelial cell proliferation and anti-apoptosis should be favorable, but the increase in vascular permeability and gene expression of a couple of procoagulant molecules, such as tissue factor, may not be. Recently, application of VEGF in experimental brain ischemia has been investigated intensively to elucidate the real effect of VEGF on the ischemic brain and to attempt to establish new therapeutic uses of VEGF in ischemic stroke.

In this study, we tried to elucidate the effects of early intraarterial infusion of low-dose vascular endothelial growth factor on ischemia/reperfusion injury after transient focal cerebral ischemia by middle cerebral artery occlusion (MCAO) in rats. We used this method of VEGF administration, that is, intraarterial infusion of low-dose VEGF, to prevent the spread of VEGF vascular responses over the whole body (e.g., hypotension and tachycardia [27]) and highlight the direct effects of VEGF on focal cerebral ischemia/reperfusion injury in situ. Ischemic cellular injury, serum extravasation, and hemorrhagic transformation after ischemia/reperfusion injury were examined pathologically and immunohistologically. In addition, MMP-2 and -9 expressions were also examined to see whether the expressions were related to the VEGF effects.

2. Materials and methods

2.1. Animal focal brain ischemia

Thirty male Sprague–Dawley (SD) rats weighing 270 to 350 g were used for this study. The rats were housed and cared for in accordance with guidance from the institutional animal care committee. Rats were anesthetized with inhaled gas (40% oxygen and 60% nitrogen mixture) containing isoflurane. The right femoral artery was cannulated for recording arterial blood pressure and collecting blood for measuring arterial blood gas. Body temperature was maintained at not less than 37.0 °C with a feedback-regulated heating blanket. Cranial temperature was measured continuously with a needle probe inserted into a temporal muscle. Focal brain ischemia was achieved by a modification of the occlusion technique originally described by Koizumi et al. [12]. Briefly, the right carotid arteries were exposed through a ventral cervical incision. A 4-0 polypropylene monofilament suture coated with silicone rubber was introduced into the internal carotid artery (ICA) via the external carotid artery to occlude the origin of the MCA. When the rats recovered from anesthesia, they were neurologically evaluated on the neurological deficit caused by the brain ischemia, as previously reported by Garcia et al. [4].

2.2. VEGF administration and reperfusion

After a 2 h ischemic state, the rats with a unilateral neurological deficit were anesthetized again for the reperfusion procedure. The suture in the ICA was withdrawn and then a polyethylene tube was cannulated into the same artery. In the VEGF group of rats (n = 15), 0.3 μg/kg of recombinant human VEGF (Sigma) in 100 μl saline was administered into the ischemic brain via the cannulated tube in the ICA. In the control group of rats (n = 15), the same volume of saline vehicle was administered. After administration, the cannulated tube was removed and antegrade reperfused blood flow was restored in the ICA. After a 1 h (n = 5 in each group), 6 h (n = 5 in each group), or 72 h (n = 5 in each group) reperfusion state, rats were subjected to histological preparation.

2.3. Histological preparation

The rats were anesthetized deeply with an intraperitoneal injection of pentobarbital and the brains were removed following transcardiac perfusion with saline and 2% paraformaldehyde in phosphate-buffered saline (PBS) (pH 7.4). Brain specimens were fixed in 4% paraformaldehyde in PBS over 24 h and subjected to standard histological processing for paraffin-embedded sections. Three-μm paraffin sections, coronally cut 4, 6, and 8 mm from the frontal pole, were used for the histopathological and immunological analyses. These three sections were placed on a glass slide together so that they could to be subjected to the following procedures under the same histopathological and immunological conditions.

2.4. Analysis of ischemic cellular injury

The area of ischemic cellular injury was estimated by the regional distribution of cells with DNA fragmentation. DNA fragmentation was detected by the incorporation of digoxigenin-dUTP with the use of DNA polymerase I, as previously reported [23]. In brief, the sections were incubated with a digoxigenin-DNA labeling mixture for 1 h, and then, incubated with horseradish peroxidase-conjugated anti-digoxigenin antibody (Boehringer Mannheim) for 1 h. The incorporation of digoxigenin-conjugated

dUTP was visualized with diaminobenzidine. The areas containing DNA-fragmented cells were traced under a microscope. These drawing areas were captured as digital images with an image scanner. The images were processed on PC-compatible computers and quantitatively measured with NIH Image software. The area of ischemic cellular injury was demonstrated as a percentage of the whole area of the three sections.

2.5. Analysis of serum extravasation

Serum extravasation was examined by immunohistochemistry with a rabbit antiserum to rat serum (Cappel Research products, NC). The area of serum extravasation was estimated by the regional distribution of positive immunoperoxidase staining. Immunoperoxidase staining was done with the streptavidin–biotin complex method using a Vectastain Elite ABC kit (Vector Laboratories). The sections were incubated with the rabbit antiserum to rat serum (1:500) for 1 h, and then incubated for 30 min with a biotinylated goat anti-rabbit IgG secondary antibody. After 30 min of incubation with streptavidin solution, streptavidin–biotin complex was visualized with diaminobenzidine. The areas containing serum extravasation were quantitatively measured with the same procedure used in the analysis of ischemic cellular injury. Furthermore, to estimate the degree of serum extravasation, we assessed the immunostaining intensity semiquantitatively by grading the intensity in 5 degrees (5: fairly strong, 4: strong, 3: moderate, 2: weak, 1: fairly weak).

2.6. Hemorrhagic transformation

The severity of hemorrhagic transformation was estimated by the number of vessels involved in hemorrhaging after hematoxylin–eosin staining. The vessels surroundedby clusters of erythrocytes were counted under a microscope.

2.7. MMP-2 and -9 expressions on vascular cells

MMP-2 and -9 expressions on vascular cells were examined to see whether the expressions were related to the hemorrhagic transformation and VEGF effects. Immunohistochemistry of MMP-2 and -9 was done in the same manner as that of the polyclonal antibody against whole rat serum. The sections were incubated with the polyclonal antibody against MMP-2 (Santa Cruz Biotechnology; 1:50) or MMP-9 (Santa Cruz Biotechnology; 1:50) for 1 h. Since MMP positive immunostaining was distributed around the border zone of ischemic cellular injury with an uneven and irregular shape, it was difficult to evaluate the area of positive immunostaining. Instead of an area measurement, we assessed the intensity of immunostaining semiquantitatively by grading the intensity in 5 degrees (5: fairly strong, 4: strong, 3: moderate, 2: weak, 1: fairly weak).

2.8. Statistical analysis

All data was expressed as the mean ± SEM. Statistical evaluation was performed using the Mann–Whitney U test. Differences were considered to be statistically significant at $P < 0.05$.

3. Results

3.1. Physiological and neurological findings

Physiological parameters, such as cranial temperature, mean arterial blood pressure, arterial partial pressure of O_2 or CO_2, and arterial blood pH, were measured in all of the rats subjected to brain ischemia at the beginning of ischemia and reperfusion. Cranial temperature and mean arterial blood pressure were elevated at the beginning of reperfusion. All parameters were not different between the VEGF and control groups (Table 1). The neurological findings were evaluated in the awake condition during the period of ischemia and after reperfusion. The neurological scores were not different between the two groups during occlusion (control 12.0 ± 0.5 vs. VEGF 12.4 ± 0.4) and after reperfusion (control 12.3 ± 0.5 vs. VEGF 12.3 ± 0.4).

3.2. Ischemic cellular injury

The area of ischemic cellular injury, estimated by DNA fragmentation (Fig. 1), increased in a reperfusion time-dependent manner. Rats with a 1 h reperfusion had no, or a very small area of ischemic cellular injury, at the basal area of the caudoputamen. Rats with a 6 h reperfusion had more areas of ischemic cellular injury than the group with 1 h of reperfusion, but still less than 5% of the total area of the

Table 1
Physiological parameters before occlusion and after reperfusion

	Control	VEGF
BT		
Before occlusion	36.9 ± 0.1	37.0 ± 0.1
After reperfusion	38.0 ± 0.3	38.2 ± 0.2
MABP (mm Hg)		
Before occlusion	87.0 ± 4.0	85.8 ± 3.8
After reperfusion	102.6 ± 5.1	98.6 ± 6.6
pH		
Before occlusion	7.40 ± 0.01	7.40 ± 0.02
After reperfusion	7.41 ± 0.01	7.42 ± 0.01
pO_2 (mm Hg)		
Before occlusion	135.0 ± 9.6	132.2 ± 8.8
After reperfusion	131.8 ± 8.4	127.7 ± 6.3
pCO_2 (mm Hg)		
Before occlusion	34.4 ± 2.6	36.4 ± 2.3
After reperfusion	33.2 ± 1.6	34.0 ± 2.2

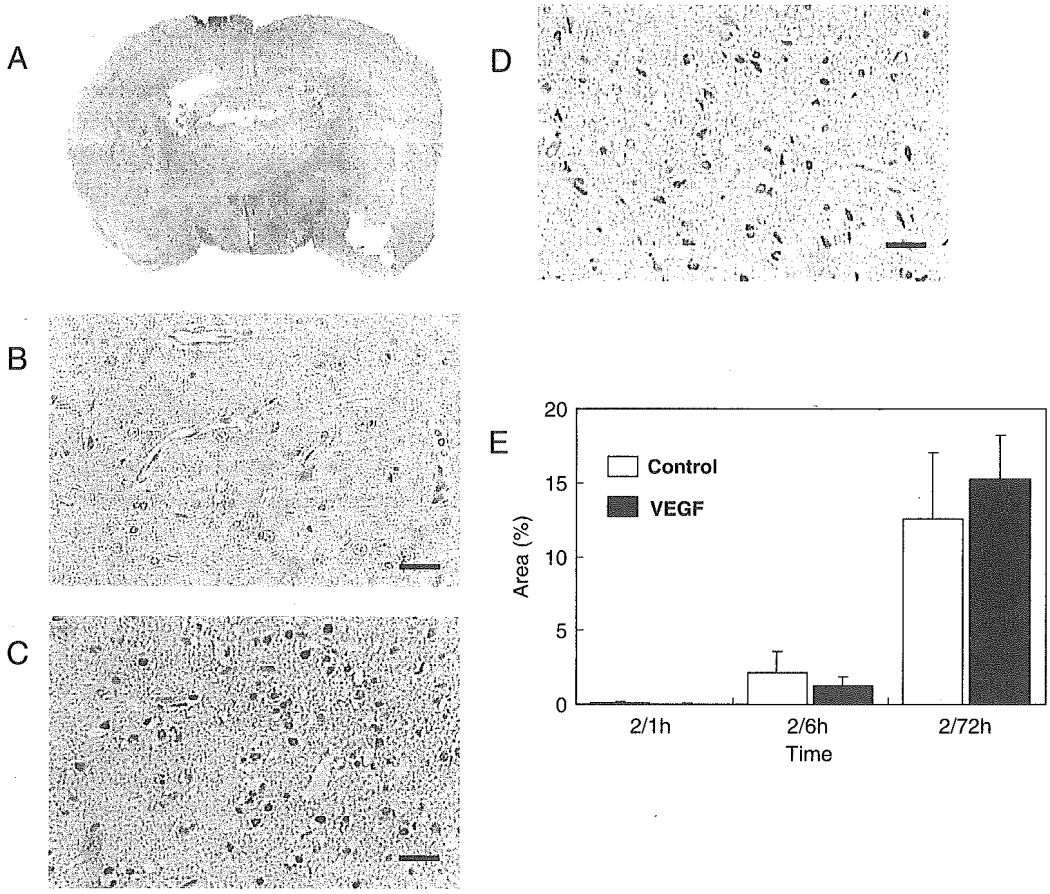

Fig. 1. Ischemic cellular injury estimated by the regional distribution of cells with DNA fragmentation. Ischemic cellular injury was extended from the caudoputamen to the cortex in a rat with a 72 h reperfusion in the control group (A). No ischemic cellular injury was detected in the no-occlusion side of a rat with a 72 h reperfusion in the control group (B). Cellular injury was distributed widely in the occlusion side of rats with a 72 h reperfusion in the control group (C) and in the VEGF group (D). A bar graph for the area of ischemic cellular injury revealed no difference in the VEGF and control groups (E). Scale bar = 20 μm.

three sections. Rats with a 72 h reperfusion showed an extension of ischemic cellular injury from the caudoputamen to the cortex, reaching to about 15% of the total area of the three sections. No difference in the area of ischemic cellular injury was observed between the VEGF and control groups for all reperfusion times (Fig. 1E).

3.3. Serum extravasation

The area of serum extravasation, estimated by immunohistochemical analysis (Fig. 2), increased from the caudoputamen to the cortex in a reperfusion time-dependent manner. The area of serum extravasation was always greater than the area of ischemic injury. The areas of serum extravasation in rats with 1-, 6-, and 72 h reperfusions were, respectively, 5, 20, and 40% of the total area of the three brain sections (Fig. 2E). Rats with a 72 h reperfusion showed serum extravasation all over the ispilateral hemisphere, and it sometimes crossed over the midline (Fig. 2A). No difference in the area of serum extravasation was observed between the VEGF and control groups for all reperfusion times (Fig. 2E). Furthermore, to assess the degree of serum extravasation, the immunostaining intensity was semiquantitatively estimated and compared with each subgroup (Table 2). There was no difference in the score between the VEGF and control groups (Table 2).

3.4. Hemorrhagic transformation

Hemorrhagic transformation, estimated by HE staining (Fig. 3), was also aggravated in a reperfusion time-dependent manner. None of the rats with a 1 h reperfusion showed hemorrhaging in either the VEGF or control group. In rats with a 6 h reperfusion, 1 rat in the control group and 3 rats in the VEGF group showed hemorrhagic transformation in a marginal zone of ischemic cellular injury. Although vessel numbers with hemorrhagic transformation were 3.6 ± 1.7 in the VEGF group and 0.4 ± 0.4 in the control group, the difference in vessel numbers was not significant ($P = 0.175$) (Fig. 3E). In rats with a 72 h reperfusion, 3 rats in the control group and all VEGF group rats showed hemorrhagic transformation in the marginal zone of ischemic cellular injury, like rats with a 6 h reperfusion. Vessel numbers with hemorrhagic transformation were significantly greater in the VEGF group than in the control group (9.4 ± 1.6 versus 2.6 ± 1.5; $P = 0.028$) (Fig. 3E). When we examined the

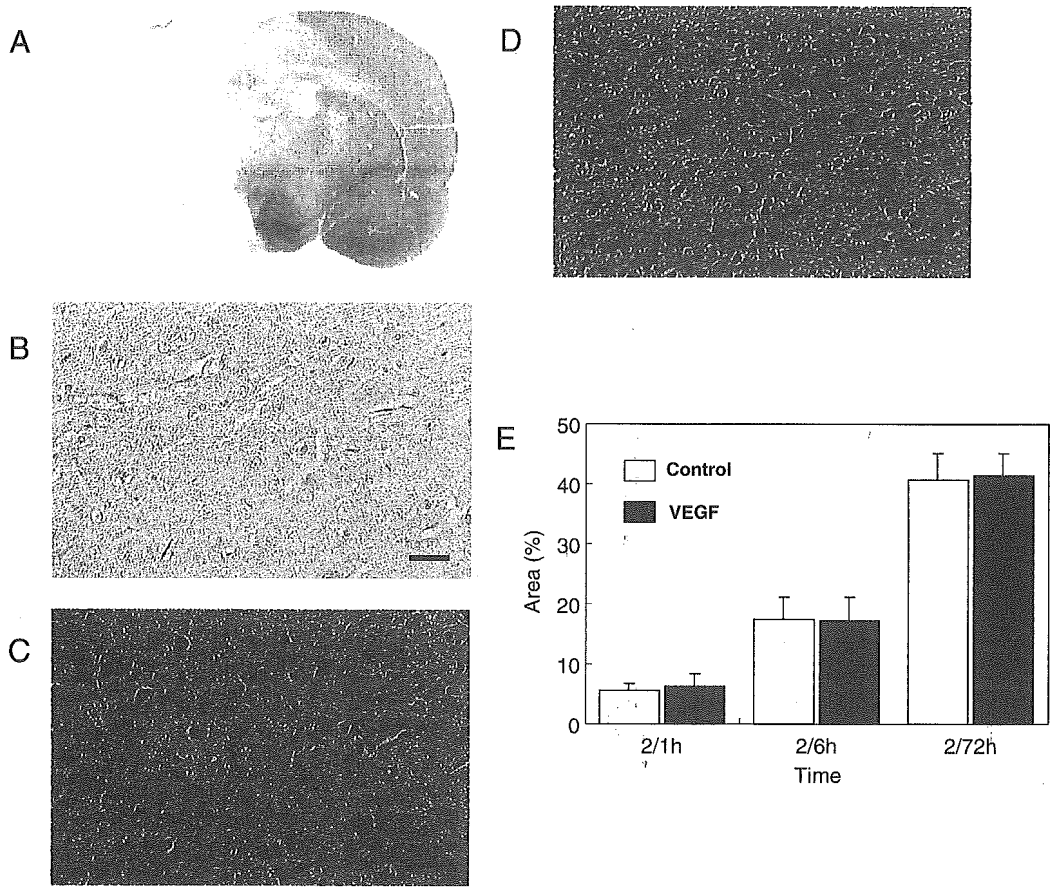

Fig. 2. Serum extravasation estimated by immunohistochemistry with a rabbit antiserum to rat serum. Serum extravasation was extended over the ispilateral hemisphere and crossed over the midline in a rat with a 72 h reperfusion in the control group (A). No serum extravasation was detected in the no-occlusion side of a rat with a 72 h reperfusion in the control group (B). Serum extravasation was distributed widely in the occlusion side of rats with a 72 h reperfusion in the control group (C) and in the VEGF group (D). A bar graph for the area of serum extravasation revealed no difference in the VEGF and control groups (E). Scale bar = 20 μm.

relationship between hemorrhagic transformation, ischemic cellular injury, and serum extravasation in rats with the same reperfusion time, an increase in hemorrhagic transformation was not always related to an increase in ischemic cellular injury or serum extravasation. Vessel number with hemorrhagic transformation was not correlated with the area of serum extravasation ($r = -0.132$), or that of ischemic cellular injury ($r = -0.293$), in rats with a 72 h reperfusion. Meanwhile, the area of ischemic cellular injury correlated well with that of serum extravasation ($r = 0.913$).

3.5. MMP-2 and -9 expressions

MMP-2 and -9 positive immunostainings were shown on microvessels and parenchymal cells near the border zone of ischemic cellular injury (Fig. 4). The intensity of immunostaining became stronger in rats with a longer reperfusion time. The intensity was semiquantitatively estimated and compared with each subgroup (Table 3). Although parenchymal cells and microvessels around the hemorrhagic transformation were frequently positive for MMP-2 and -9 immunostainings, the intensity was not enhanced in the VEGF group compared with the control group (Table 3).

Table 2
Semiquantitative analysis of the degree of serum extravasation

	Control	VEGF
2/1 h	2.0 ± 1.0	2.4 ± 0.9
2/6 h	3.6 ± 1.5	3.0 ± 0.7
2/72 h	4.2 ± 0.8	4.6 ± 0.5

4. Discussion

We demonstrated that the early intraarterial infusion of low-dose VEGF aggravated hemorrhagic transformation in acute brain ischemia/reperfusion injury. We used this method of VEGF administration to highlight the localized direct effects of VEGF on brain ischemia without hypotension and tachycardia as the general effects of VEGF. A study focusing on the effects of VEGF on hemodynamics and cardiac performance showed that intravenous injection of VEGF at a dose of 1 μg/kg decreased mean arterial pressure and increased heart rate [26]. Therefore, we

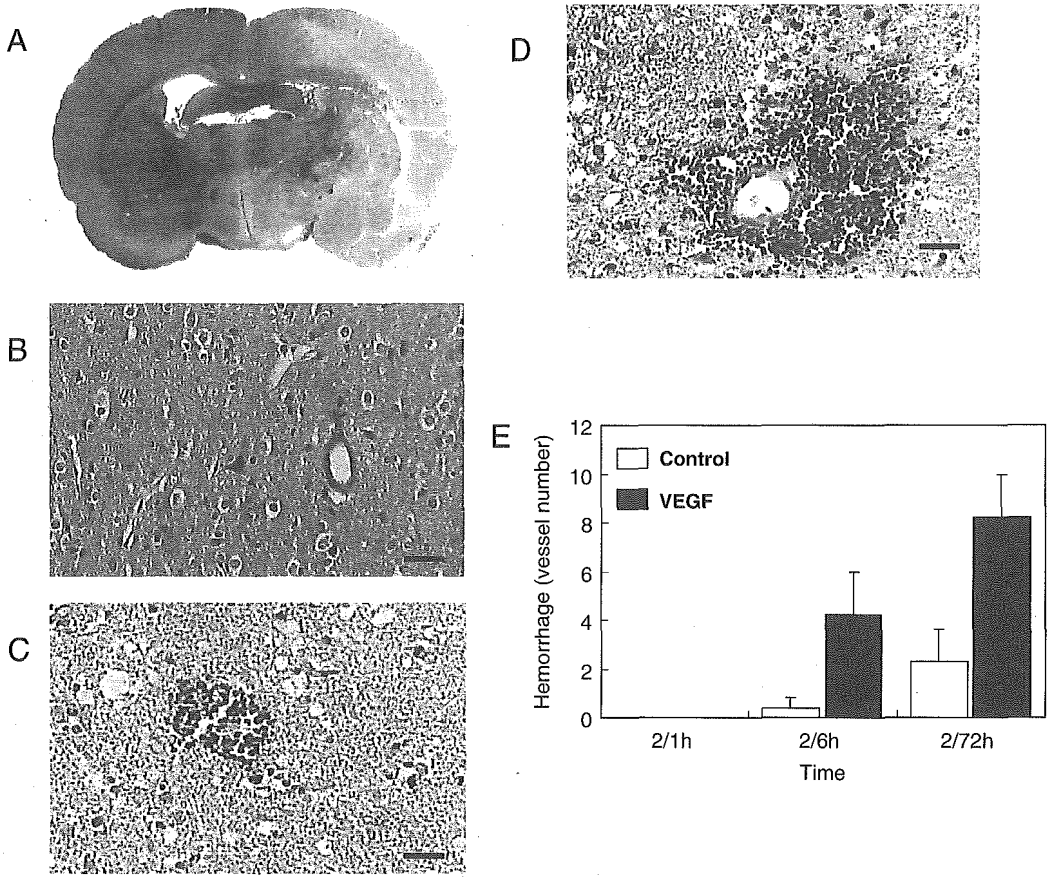

Fig. 3. Hemorrhagic transformation estimated by HE staining. Hemorrhagic transformation was detected around the marginal zone of ischemic cellular injury in a rat with a 72 h reperfusion in the control group (A). No hemorrhagic transformation was detected in the no-occlusion side of a rat with a 72 h reperfusion in the control group (B). Hemorrhagic transformation was detected in the occlusion side of rats with a 72 h reperfusion in the control group (C) and in the VEGF group (D). A bar graph for vessel numbers in hemorrhagic transformation revealed that the vessel numbers were significantly greater in the VEGF group than in the control group, for rats with a 72 h reperfusion ($P < 0.05$), but not for rats with a 6 h reperfusion ($P = 0.175$). Scale bar = 20 μm.

examined the effects of VEGF on hemodynamic parameters with doses under 1 μg/kg in a pilot study (data not shown), and then we determined the VEGF dose as 0.3 μg/kg because we observe no responses of hypotension and tachycardia with this dose. This dose is over three-thousand-times lower than the dose of 1 mg/kg used in a previous study which reported that intravenously infused VEGF enhanced angiogenesis and promoted blood–brain barrier leakage in the ischemic brain [28].

Since one of the main functions of VEGF is to increase vascular permeability, it is reasonable to think that the extension of vascular permeability would be related to hemorrhagic transformation. However, at least using the VEGF dose applied in this study, VEGF could not enlarge the area of serum extravasation (Fig. 2C). The correlation analysis in this study showed that the vessel number of hemorrhagic transformation was not correlated with the area of ischemic injury or that of serum extravasation. Furthermore, semiquantitative analysis of the degree of serum extravasation demonstrated that there was no difference between VEGF and control groups. Therefore, in this study, an increase in vascular permeability was not directly responsible for the increased hemorrhagic transformation in the VEGF group.

MMPs have been associated with hemorrhagic transformation in experimental models of cerebral ischemia. Heo et al. demonstrated the early potential role of MMP-2 in neuronal injury, and an association of MMP-9 with hemorrhagic transformation after focal cerebral ischemia [9]. Sumii et al. demonstrated MMP-9 was upregulated in the rat ischemic brain with hemorrhagic transformation, with this upregulation being significantly higher in tPA-treated rats than in untreated controls [21]. In this study, we demonstrated that MMP-2 and MMP-9 were expressed on parenchymal cells and microvessels near the border zone of ischemic cellular injury (Fig. 4). However, the expression was not enhanced in the VEGF group compared with the control group. Therefore, the increased hemorrhagic transformation in this study did not seem to be induced by MMP overexpression.

The control group with a 72 h reperfusion in this study showed hemorrhaging of microvessels in the ischemia/reperfusion area with a rate of 60% (3/5). This finding means that the onset of hemorrhage, that is, the breakdown

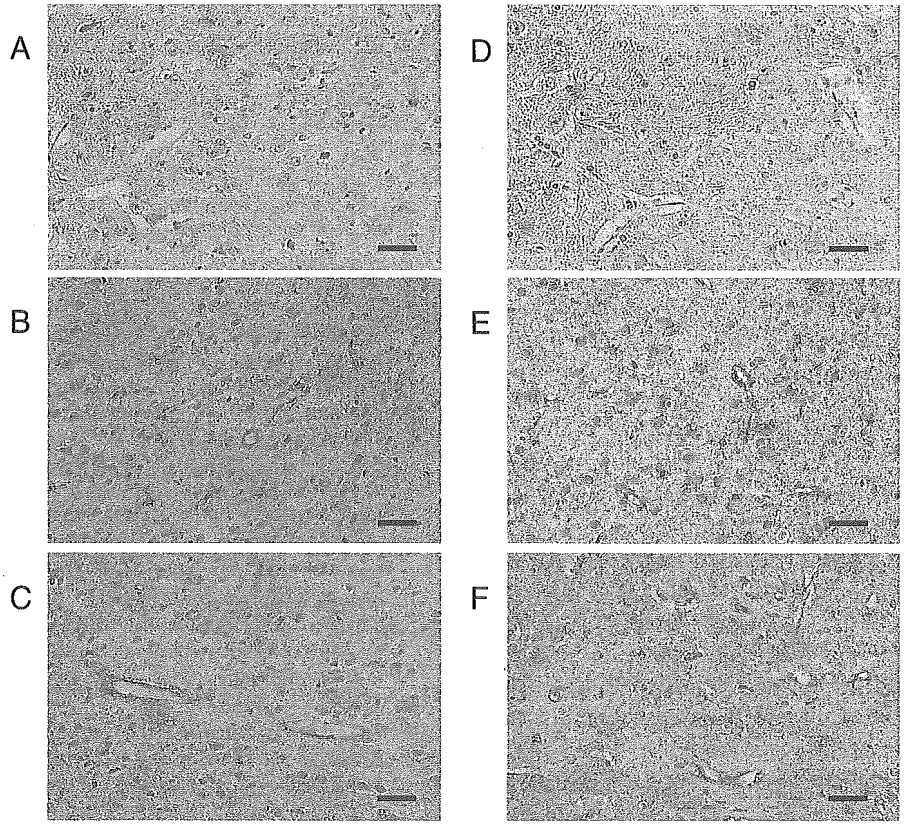

Fig. 4. Immunohistochemistry of MMP-2 and -9. No positive immunostaining of MMP-2 was detected in the no-occlusion side of a rat with a 72 h reperfusion in the control group (A). Positive immunostaining of MMP-2 was detected on microvessels and parenchymal cells near the border zone of ischemic cellular injury in the control group (B) and in the VEGF group (C). No positive immunostaining of MMP-9 was detected in the no-occlusion side of a rat with a 72 h reperfusion in the control group (D). Positive immunostaining of MMP-9 was detected on microvessels and parenchymal cells near the border zone of ischemic cellular injury in the control group (E) and in the VEGF group (F). Scale bar = 20 μm.

of vascular integrity, happened without the influence of exogenous VEGF. A 2 h ischemia with reperfusion seems to be severe enough to deteriorate the vascular integrity of the brain microvessels, resulting in minor leakage. Therefore, exogenous VEGF administered intravascularly may accelerate blood extravasation in injured microvessels with minor leakage. In spite of the limitations of the present study, that is, the lack of the estimation of blood flow, we speculate that localized vasodilatation may be a potential cause of vascular leakage acceleration. It has been demonstrated that VEGF induces vasodilatation in a dose-dependent fashion [5] and dominantly in microvessels in comparison with systemic arteries and veins [13].

The function of VEGF in the ischemic brain has been investigated by experiments with recombinant VEGF, antibodies neutralizing VEGF, or VEGF transgenic animals.

Table 3
Semiquantitative analysis of MMP-2 and -9 immunostainings

	MMP-2		MMP-9	
	Control	VEGF	Control	VEGF
2/1 h	1.4 ± 0.5	1.2 ± 0.4	1.6 ± 0.9	1.6 ± 0.5
2/6 h	2.4 ± 0.5	2.2 ± 0.8	2.0 ± 0.7	2.2 ± 0.8
2/72 h	3.0 ± 0.7	3.2 ± 0.8	3.2 ± 0.8	2.8 ± 0.9

These studies have explored whether VEGF has beneficial or harmful effects on the ischemic brain. Hayashi et al. demonstrated that treatment with topical VEGF application on the brain surface significantly reduced infarct volume and edema formation [8]. Comparable beneficial effects of VEGF were demonstrated when VEGF was infused into the lateral ventricle of the ischemic brain [7,22]. Ventricular VEGF infusion induced angiogenesis in the penumbra area of the rat brain ischemic model, as well as reduced infarct size [22]. Late postischemic (24 h) intravenous administration of recombinant VEGF to ischemic rats also enhanced angiogenesis in the ischemic penumbra and significantly improved neurological recovery [28]. In this study, we could not detect an increase in vessels, that is, evidence of angiogenesis, in any rats with VEGF administration (data not shown); this was probably due to the fact that the early infusion of VEGF and early estimation of ischemia/reperfusion injury were employed. Meanwhile, it has been demonstrated in the rat brain ischemic model that neuroprotection of ischemic brains by exogenous VEGF does not necessarily occur simultaneously with angiogenesis [16]. Following transient MCAO in transgenic mice overexpressing human VEGF165, VEGF overexpression provided neuroprotection reflected by the smaller infarct volume

and reduced disseminated neuronal injury, although regional blood flow was decreased due to hemodynamic steal phenomena in ischemic areas [25]. The neuroprotective effect of VEGF was demonstrated in an in vitro study which reported that VEGF approximately doubled the number of cultured neurons surviving after hypoxia and glucose deprivation [11]. Therefore, even if angiogenesis has a beneficial role on the ischemic brain, the neuroprotective effects of VEGF seem to be partly independent of angiogenesis. The harmful effects of VEGF were also demonstrated in an animal model of brain ischemia. Inhibition of VEGF activity by neutralizing antibodies significantly reduced edema formation and tissue damage, indirectly suggesting that VEGF has harmful effects on brain ischemia [24,20]. Early postischemic (1 h) administration of VEGF to ischemic rats significantly increased blood–brain barrier leakage, hemorrhagic transformation, and ischemic lesions [28]. Therefore, the harmful effects of VEGF depend on an increase in vascular permeability and hemorrhagic transformation.

Considering the abovementioned findings and our experimental findings, how VEGF acts on brain ischemia depends on time and the method of VEGF application. VEGF seems to enhance the increased permeability and destructive changes to vascular integrity when VEGF reaches vascular beds directly in the early phase of ischemia/reperfusion. Meanwhile, VEGF seems to enhance neuroprotection and/or angiogenesis when VEGF reaches ischemic neuronal tissues in a transparenchymal way or in a relatively late phase of ischemia/reperfusion. We have to consider these VEGF characteristics when we establish new therapeutic uses of VEGF for ischemic stroke.

In conclusion, our findings show that early intraarterial infusion of low-dose VEGF aggravates hemorrhagic transformation in ischemia/reperfusion injury. The aggravated hemorrhagic transformation does not seem to depend on the enlargement of ischemic cellular injury, serum extravasation, or overexpressions of MMP-2 and -9. Although further studies are needed to explore the mechanism of aggravated hemorrhagic transformation, we speculate that VEGF causes vasodilatation in the injured microvessels with minor leakage, resulting in the acceleration of hemorrhagic transformation.

Acknowledgments

This study was supported in part by a Grant-in-Aid for Scientific Research from the Japan Society for the Promotion of Science and by a research grant for Cardiovascular Diseases 15C-1 from the Ministry of Health, Labor, and Welfare of Japan.

References

[1] T. Abumiya, J. Lucero, J.H. Heo, M. Tagaya, J.A. Koziol, B.R. Copeland, G.J. del Zoppo, Activated microvessels express vascular endothelial growth factor and integrin αvβ3 during focal cerebral ischemia, J. Cereb. Blood Flow Metab. 19 (1999) 1038–1050.

[2] G.J. del Zoppo, J.M. Hallenbeck, Advances in the vascular pathophysiology of ischemic stroke, Thromb. Res. 98 (2000) 73–81.

[3] N. Ferrara, H.P. Gerber, LeCouter, The biology of VEGF and its receptors, J. Nat. Med. 9 (2003) 669–676.

[4] J.H. Garcia, S. Wagner, K.F. Liu, X.J. Hu, Neurological deficit and extent of neuronal necrosis attributable to middle cerebral artery occlusion in rats. Statistical validation, Stroke 26 (1995) 627–634.

[5] T.R. Grover, J.P. Zenge, T.A. Parker, S.H. Abman, Vascular endothelial growth factor causes pulmonary vasodilation through activation of the phosphatidylinositol-3-kinase-nitric oxide pathway in the late-gestation ovine fetus, Pediatr. Res. 52 (2002) 907–912.

[6] G.F. Hamann, Y. Okada, G.J. del Zoppo, Hemorrhagic transformation and microvascular integrity during focal cerebral ischemia/reperfusion, J. Cereb. Blood Flow Metab. 16 (1996) 1373–1378.

[7] M.R. Harrigan, S.R. Ennis, S.E. Sullivan, R.F. Keep, Effects of intraventricular infusion of vascular endothelial growth factor on cerebral blood flow, edema, and infarct volume, Acta Neurochir. (Wien) 145 (2003) 49–53.

[8] T. Hayashi, K. Abe, Y. Itoyama, Reduction of ischemic damage by application of vascular endothelial growth factor in rat brain after transient ischemia, J. Cereb. Blood Flow Metab. 18 (1998) 887–895.

[9] J.H. Heo, J. Lucero, T. Abumiya, J.A. Koziol, B.R. Copeland, G.J. del Zoppo, Matrix metalloproteinases increase very early during experimental focal cerebral ischemia, J. Cereb. Blood Flow Metab. 19 (1999) 624–633.

[10] W.C. Jean, S.R. Spellman, E.S. Nussbaum, W.C. Low, Reperfusion injury after focal cerebral ischemia: the role of inflammation and the therapeutic horizon, Neurosurgery 43 (1998) 1382–1396.

[11] K.L. Jin, X.O. Mao, D.A. Greenberg, Vascular endothelial growth factor: direct neuroprotective effect in in vitro ischemia, Proc. Natl. Acad. Sci. U. S. A. 97 (2000) 10242–10247.

[12] J. Koizumi, Y. Yoshida, T. Nakazawa, G. Ooneda, Experimental studies of ischemic brain edema: 1. A new experimental model of cerebral embolism in rats in which recirculation can be introduced in the ischemic area, Jpn. J. Stroke 8 (1986) 1–8.

[13] R.J. Laham, J. Li, M. Tofukuji, M. Post, M. Simons, F.W. Sellke, Spatial heterogeneity in VEGF-induced vasodilation: VEGF dilates microvessels but not epicardial and systemic arteries and veins, Ann. Vasc. Surg. 17 (2003) 245–252.

[14] V. Larrue, R.R. von Kummer, A. Muller, E. Bluhmki, Risk factors for severe hemorrhagic transformation in ischemic stroke patients treated with recombinant tissue plasminogen activator: a secondary analysis of the European–Australasian Acute Stroke Study (ECASS II), Stroke 32 (2001) 438–441.

[15] M.Y. Lee, W.K. Ju, J.H. Cha, B.C. Son, M.H. Chun, J.K. Kang, C.K. Park, Expression of vascular endothelial growth factor mRNA following transient forebrain ischemia in rats, Neurosci. Lett. 265 (1999) 107–110.

[16] P.S. Manoonkitiwongsa, R.L. Schultz, D.B. McCreery, E.F. Whitter, P.D. Lyden, Neuroprotection of ischemic brain by vascular endothelial growth factor is critically dependent on proper dosage and may be compromised by angiogenesis, J. Cereb. Blood Flow Metab. 24 (2004) 693–702.

[17] J. Montaner, J. Alvarez-Sabin, C.A. Molina, A. Angles, S. Abilleira, J. Arenillas, Monasterio, Matrix metalloproteinase expression is related to hemorrhagic transformation after cardioembolic stroke, J. Stroke 32 (2001) 2762–2767.

[18] K.H. Plate, H. Beck, S. Danner, P.R. Allegrini, C. Wiessner, Cell type specific upregulation of vascular endothelial growth factor in an MCA-occlusion model of cerebral infarct, J. Neuropathol. Exp. Neurol. 58 (1999) 654–666.

[19] C. Ruhrberg, Growing and shaping the vascular tree: multiple roles for VEGF, BioEssays 25 (2003) 1052–1060.
[20] H.J. Schoch, S. Fischer, H.H. Marti, Hypoxia-induced vascular endothelial growth factor expression causes vascular leakage in the brain, Brain 125 (2002) 2549–2557.
[21] T. Sumii, E.H. Lo, Involvement of matrix metalloproteinase in thrombolysis-associated hemorrhagic transformation after embolic focal ischemia in rats, Stroke 33 (2002) 831–836.
[22] Y. Sun, K. Jin, L. Xie, J. Childs, X.O. Mao, A. Logvinova, D.A. Greenberg, VEGF-induced neuroprotection, neurogenesis, and angiogenesis after focal cerebral ischemia, J. Clin. Invest. 111 (2003) 1843–1851.
[23] M. Tagaya, K.F. Liu, B. Copeland, D. Seiffert, R. Engler, J.H. Garcia, G.J. del Zoppo, DNA scission after focal brain ischemia. Temporal differences in two species, Stroke 28 (1997) 1245–1254.
[24] N. van Bruggen, H. Thibodeaux, J.T. Palmer, W.P. Lee, L. Fu, B. Cairns, D. Tumas, R. Gerlai, S.P. Williams, M. van Lookeren Campagne, N. Ferrara, VEGF antagonism reduces edema formation and tissue damage after ischemia/reperfusion injury in the mouse brain, J. Clin. Invest. 104 (1999) 1613–1620.
[25] Y. Wang, E. Kilic, U. Kilic, B. Weber, C.L. Bassetti, H.H. Marti, D.M. Hermann, VEGF overexpression induces post-ischaemic neuroprotection, but facilitates haemodynamic steal phenomena, Brain 128 (Pt. 1) (2005) 52–63.
[26] R. Yang, G.R. Thomas, S. Bunting, A. Ko, N. Ferrara, B. Keyt, J. Ross, H. Jin, Effects of vascular endothelial growth factor on hemodynamics and cardiac performance, J. Cardiovasc. Pharmacol. 6 (1996) 838–844.
[27] R. Yang, A.K. Ogasawara, T.F. Zioncheck, Z. Ren, G.W. He, G.G. De Guzman, N. Pelletier, B.Q. Shen, S. Bunting, H. Jin, Exaggerated hypotensive effect of vascular endothelial growth factor in spontaneously hypertensive rats, Hypertension 39 (2002) 815–820.
[28] Z.G. Zhang, L. Zhang, Q. Jiang, R. Zhang, K. Davies, C. Powers, N. Bruggen, Chopp M VEGF enhances angiogenesis and promotes blood–brain barrier leakage in the ischemic brain, J. Clin. Invest. 106 (2000) 829–838.

□ ORIGINAL ARTICLE □

Transoral Carotid Ultrasonography for Evaluating Internal Carotid Artery Occlusion

Katsunori ISA, Masahiro YASAKA, Kazumi KIMURA, Kazuyuki NAGATSUKA and Kazuo MINEMATSU

Abstract

Background and Purpose **Transoral carotid ultrasonography (TOCU) has enabled the assessment of the distal portion of the extracranial internal carotid artery (ICA). We evaluated the ultrasonographic features of ICA occlusion using TOCU.**

Methods **We studied 50 occluded ICAs in 42 stroke patients. The mechanism of ICA occlusion was embolic (group E) in 14 arteries and thrombotic (group T) in the other 36 arteries. We used a color flow imaging system equipped with special convex array transducers, and placed the probe on the postero-lateral pharyngeal wall to identify the distal extracranial ICA. We evaluated intraluminal echodensity (lucent or opaque) and measured the diameter of the ICA. Then, we examined the relationship of these early (<1 week after onset) and chronic (>4 weeks after onset) phase TOCU findings to the mechanism of ICA occlusion and the site of occlusion.**

Results **In the early phase of a stroke, the intraluminal echodensity was more frequently lucent (9/11, 81.8%) in group E than in group T (5/20, 20%, $p<0.05$). In the chronic phase, echodensity became opaque in both groups. In the early phase, the lucent echodensity was more frequently seen in patients with distal occlusion than in those with proximal occlusion. Thus, it may represent blood or fresh thrombus formation. In patients with unilateral ICA occlusion, the occluded ICA was significantly smaller in diameter than the non-occluded contralateral artery both in the early and chronic phases.**

Conclusion **The echodensity and diameter of the extracranial ICA distal portion as found on TOCU can help to identify the mechanism of ICA occlusion.**
(Internal Medicine 44: 567–571, 2005)

Key words: internal carotid artery (ICA), transoral carotid ultrasonography (TOCU)

Introduction

Conventional carotid ultrasonographic assessment of the distal extracranial internal carotid artery (ICA) is limited by the mandibular bone, even in patients with a low bifurcation. In addition, far distal segments in the skull before the petrous portion are often affected by the pathological process, such as dissection, fibromuscular dysplasia, stationary artery waves, and hypoplasia of the ICA (1).

The mechanism of the ICA occlusion, embolic or thrombotic occlusion, has usually been estimated by temporal profile of stroke, neuroradiological features, risk factors of atherosclerosis, electrocardiography or echocardiography. It was, however, often difficult to distinguish because patients with ICA occlusion often have not only heart diseases but also risk factors of atherosclerosis. Therefore, evaluation of the extracranial distal ICA by ultrasonography may provide further helpful information in diagnosing the mechanism of the ICA occlusion.

We previously reported the usefulness of transoral carotid ultrasonography (TOCU) in evaluating the distal portion of the extracranial ICA (2, 3). Recently, Kishikawa et al (4) reported findings of carotid severe stenosis before and after carotid endarectomy by using TOCU that can be obtained neither by conventional carotid ultrasonography nor by angiography. In the acute phase of a stroke with ICA occlusion, it is important to distinguish between embolic and atherothrombotic etiology as early as possible. Knowledge of the particular etiology determines the treatment and allows further deterioration to be prevented in atherothrombotic stroke (5, 6). Furthermore, appropriate secondary prevention differs, depending on the etiology (7). Therefore, we investigated the ultrasonographic findings found on TOCU to determine which findings help to distinguish between embolic and thrombotic ICA occlusion.

From the Cerebrovascular Division, Department of Medicine, National Cardiovascular Center, Osaka
Received for publication March 30, 2004; Accepted for publication January 11, 2005
Reprint requests should be addressed to Dr. Katsunori Isa, the Third Internal Medicine, School of Medicine, University of the Ryukyus, 207 Uehara, Nishihara, Okinawa 903-0215

Subjects and Methods

Patients

We studied 50 occluded ICAs in 42 stroke patients (34 men and 8 women; age 64.9±12.4 years). ICA occlusion was confirmed by conventional cerebral angiography, magnetic resonance angiography. Cases of carotid pseudocclusion were excluded. There were 8 cases with bilateral ICA occlusion and 34 cases with unilateral ICA occlusion.

Diagnosis of carotid occlusion

We classified the subjects into two groups according to ICA occlusion mechanisms. Thus, there was the embolic group and the thrombotic group. The diagnosis of embolic stroke was made if the patient met at least 2 of the following 3 criteria: 1) a sudden onset of clinical symptoms with a focal neurologic deficit at the time of onset; 2) the presence of a certain source of cardiac emboli including valvular heart disease, acute myocardial infarction, atrial fibrillation, sick sinus syndrome, or prosthetic valves; 3) evidence of embolization in other parts of the body. A thrombotic stroke was diagnosed when patients had risk factors of atherosclerosis such as hypertension, diabetes mellitus, or dyslipidemia, and did not have any source of emboli as in embolic group.

Previously diagnosed hypertension, diabetes mellitus and hypercholesterolemia were considered atherosclerotic risk factors. Patients taking antihypertensive medicine and with a systolic blood pressure ≧140 mmHg or diastolic blood pressure ≧90 mmHg were considered hypertensive, while diabetic patients were defined as those taking insulin or oral antidiabetic agents, and exhibiting a fasting plasma glucose level of ≧126 mg/dl or plasma glucose at any time of ≧200 mg/dl. Patients taking antihypercholesterolemic medicine, or with a plasma total cholesterol of ≧220 mg/dl were defined as having hypercholesterolemia.

Transoral carotid ultrasonography (TOCU)

TOCU was performed by a stroke physician (K.I.) in the early (<1 week after onset) and the chronic (>4 weeks after onset) phases. We used a color flow imaging system (ATL Ultramark 9, ATL Ultrasound Inc., Bothell, USA) equipped with a special convex array transducer (9-5 ICT), and placed the probe on the pharyngeal posterolateral wall to identify the distal extracranial ICA. We evaluated the intraluminal echodensity and classified it as lucent or opaque (Fig. 1). In cases where the occluded ICA lumen can be visualized in B-mode with increasing echodensity, we diagnosed its intraluminal echodensity 'opaque'. On the other hand, we classified occluded ICA lumen to be visualized without increasing echodensity 'lucent'.

Evaluation of carotid occlusion

A lucent echodensity likely represents blood or fresh thrombus formation. We also measured the diameter of the ICA distal cervical portion (C3 level). We then, studied the relationship of these TOCU findings to the duration from stroke onset to TOCU examination, mechanism of ICA occlusion, and site of occlusion (proximal or distal portion of the ICA). The degree of echodensity and the measurement of the diameter of the extracranial ICA distal portion by TOCU was analyzed in this way so as to determine if the mechanism of ICA occlusion could be identified using these parameters.

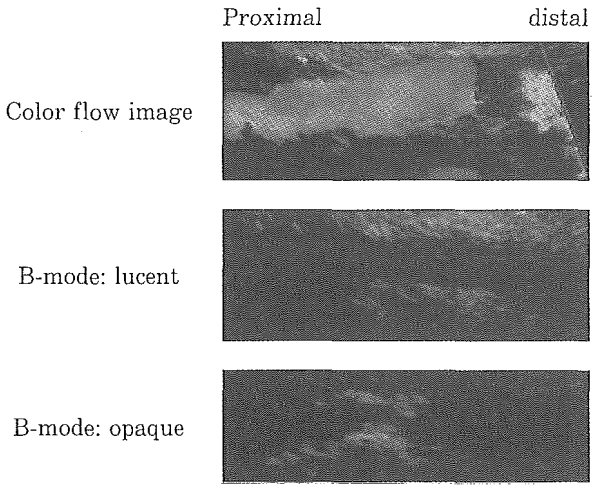

Figure 1. Transoral carotid ultrasonography (TOCU) findings of the distal portion of extracranial internal carotid artery (ICA). Upper; B-mode with color flow image of normal ICA. Middle; B-mode image indicating lucent area inside the ICA. Lower; B-mode image showing partial opaque area inside the ICA.

Stastical method

Associations between baseline characteristics and ICA diameter of study groups were analyzed by χ^2 stastistics. Findings of ICA intraluminal echodensity were analyzed by paired t-test. We chose a value of p=0.05 as the level of statistical significance.

Results

The characteristics of the two groups with ICA occlusion are summarized in Table 1. Hypertension and diabetes mellitus were more frequently seen in the thrombotic group than in the embolic group. Atrial fibrillation was more common in the embolic group. Distal ICA occlusion was more frequently seen in the embolic group (8/14) than in the thrombotic group (5/36, p<0.005).

Inside the ICA at the site of occlusion in both groups, no color flow images were obtained and doppler wave form demonstrated only a systolic small spike which was compatible with arterial occlusion.

In the early phase of a stroke, intraluminal echodensity was more frequently lucent (9/11) in the embolic group than in the thrombotic group (5/20, p<0.05, Table 2a). Intra-

Table 1. Characteristics of Study Groups

Group	Embolic (n=12)	Thrombotic (n=30)	p value
Men, n (%)	9 (75)	25 (83.3)	
Age, y	68.7±14.2	63.6±11.7	ns
Hypertension, n (%)	4 (33.3)	23 (76.7)	<0.05
Diabetes mellitus, n (%)	2 (16.7)	16 (53.3)	<0.05
Hyperlipidemia, n (%)	6 (50)	16 (53.3)	ns
Smoking, n (%)	5 (41.7)	20 (66.7)	ns
Atrial fibrillation, n (%)	7 (58.3)	2 (6.7)	<0.0005
Other heart disease, n (%)	8 (66.7)	8 (26.7)	ns
Stroke history, n (%)	2 (16.7)	10 (33.3)	ns
Sites of ICA occlusion			
Early phase			
Distal	7	3	
Proximal	4	17	
Chronic phase			
Distal	1	2	
Proximal	2	14	
Total	14	36	

Table 2. Evaluation of Intraluminal Echodensity

a) Early phase

	Embolic	Thrombotic	
Lucent	9	5	
Opaque	2	15	p<0.05
	Proximal	Distal	
Lucent	7	7	
Opaque	14	3	p<0.05

b) Chronic phase

	Embolic	Thrombotic	
Lucent	0	1	
Opaque	3	15	n.s.
	Proximal	Distal	
Lucent	1	0	
Opaque	15	3	n.s.

luminal echodensity was more frequently opaque (14/21) with the occlusion of the proximal ICA (3/10, p<0.05). On the other hand, in the chronic phase in patients with a distal ICA occlusion, echodensity was almost always opaque in both the embolic (3/3) and the thrombotic (15/16) groups (Table 2b).

In one case with distal occlusion in the embolic group, intraluminal echodensity was lucent during the first day of occlusion. On the third day, the intermediate echo substance appeared at the petrous side of the cervical distal ICA. On the 30th day of occlusion, the whole intraluminal echodensity of the occluded ICA became opaque (Fig. 2).

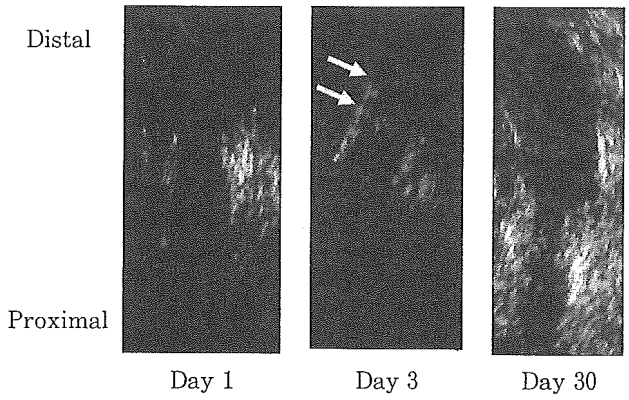

Figure 2. Serial TOCU findings in a case of distal ICA embolic occlusion. Upper (day 1); intraluminal echodensity was lucent. Middle (day 3); the intermediate echo substance (arrow) appeared at the petrous side of the cervical distal ICA. Lower (day 30); the whole intraluminal echodensity of the occluded ICA became opaque.

Comparing the 2 groups in the early phase of a stroke, the occluded ICA had a significantly smaller diameter than that of the normal contralateral ICA in the thrombotic group (3.9±1.6 mm vs 4.9±0.7 mm, p<0.05, Table 3), but there was no significant difference in the embolic group (4.2±0.9 vs 4.7±0.7, n.s.). In the chronic phase, the 3 occluded ICAs in the embolic group were too opaque to allow for identification. In the chronic phase, the occluded ICA of the thrombotic group had a significantly smaller diameter than

Table 3. Evaluation of ICA Diameter

a) Early phase

	Occlusion site	Non-occluded site	p value
Embolic (n=11, mm)	4.2±0.9	4.7±0.7	ns
Thrombotic (n=20, mm)	3.9±1.6	4.9±0.7	<0.05
Total (n=31, mm)	4.0±1.1	4.8±0.8	<0.05

b) Chronic phase

	Occlusion site	Non-occluded site	p value
Embolic (n=3, mm)	*	4.1±0.8	–
Thrombotic (n=16, mm)	3.8±1.5	4.9±0.4	<0.05

*All 3 arteries were too opaque to identify.

the contralateral ICA (3.8±1.5 vs 4.9±0.4, $p<0.05$, Table 3b).

Discussion

In the embolic group, echodensity was lucent at the onset of the ICA occlusion and became opaque in the chronic phase, suggesting that the presence of blood in the acute phase and retrograde thrombus formation subsequently. In the thrombotic group, the lumen of the ICA was filled with an opaque echogenic substance in the acute phase of occlusion. This echogenic substance likely represents the atherosclerotic mechanism of the occlusion. This substance is typically observed at the origin of the ICA (8). In the early phase of the thrombotic group, the intraluminal echodensity was not always opaque. There might be two reasons. One of them is the mechanism of thrombotic ICA occlusion. When the ICA is occluded due to gradual development of plaque thickness, the intraluminal echodensity in the acute phase may be opaque. However, when ICA flow is stopped abruptly by plaque rupture, the intraluminal echodensity may be lucent. The second reason may be due to the accuracy of diagnosing mechanism of ICA occlusion. We might misdiagnose the ICA occlusion due to embolic mechanism as that caused by thrombotic mechanism.

In the thrombotic group, the diameter of the occluded ICA in the acute phase of occlusion was already decreased as compared to the normal side. This finding would indicate that the ICA occlusion was not sudden, but gradual, progressing to severe stenosis and decreased blood flow. On the other hand, in the embolic group, the ICA occlusion was sudden, and the ICA diameter was not decreased, because counter blood flow from the distal ICA was preserved at this time.

Since the therapy of an acute stroke depends on the etiology of the ICA occlusion, TOCU can be used to determine the mechanism of the ICA occlusion. This is especially true with serial observations of intraluminal echodensity of the ICA. TOCU showed lucency in the acute phase, which became opaque in distal embolic ICA occlusion. Even in the early phase of ICA occlusion, there were differences in TOCU findings between embolic and thrombotic groups. In the thrombotic group, the thrombotic occluded ICA diameter decreased and had an opaque intraluminal echodensity. The embolic occluded ICA diameter did not decrease and no intraluminal opaque echodensity was seen. However, with time most of the occluded ICAs decreased in diameter and the intraluminal echodensity became opaque.

While distal ICA occlusion was more frequent in the embolic group, proximal ICA occlusion was more frequent in the thrombotic group. Embolic substances tended to cluster in the distal portion of the ICA in the embolic group, while almost all the cases in the thrombotic group had atherosclerotic change in the proximal portion of the ICA.

TOCU findings enable us to determine the mechanism of the occlusion of the internal carotid artery. We found opaque echodensity substances in acute thrombotic occlusions, which would be consistent with atherothrombotic substances such as plaques and attached thrombus. In acute embolic occlusion, echolucent material filled the vascular lumen. In fact, it could hardly be differentiated on the gray scale from blood flow in a patent ICA. We suggest that this lucent echodensity represents blood or fresh thrombus formation.

In one case with distal occlusion in the embolic group, we noted a high echodensity opaque intraluminal substance in the distal ICA. It has been reported that when angiography is performed during the 1st or 2nd day, a tailing off appearance of a column of contrast material in the proximal artery is suggestive of retrograde thrombus extension from the occlusion of the supraclinoid ICA (9). Therefore, we conclude that the finding in this case represents a retrograde thrombus.

Conclusion

This study revealed that TOCU findings can help to confirm and establish the etiology and location of the lesion in a stroke patient. Since etiology determines early treatment, TOCU findings can help guide the management of such patients.

Acknowledgements and Funding: This study was supported in part by research grants for cardiovascular disease (12C-2, 12A-1 and 14-C) from the Ministry of Health, Labor and Welfare of Japan and by the Special Coordination Funds for Promoting Science and Technology (Strategic Promotion System for Brain Science) from the Science and Technology Agency of Japan.

References

1) Mohr JP, Gautier JC, Pessin MS. Internal carotid artery disease in: Stroke: Pathophysiology, Diagnosis, and Management 3rd ed. Barnett HJM, Mohr JP, Stein BM, Yatsu FM, eds. Phyladelphia, Churchill Livingstone, 1998: 355–400.
2) Yasaka M, Kimura K, Otsubo R, et al. Transoral carotid ultrasono-

graphy. Stroke **29**: 1383–1388, 1998.
3) Koga M, Kimura K, Minematsu K, Yasaka M, Isa K, Yamaguchi T. Transoral carotid ultrasonographic findings in internal carotid artery d issection—a case report. Angiology **8**: 699–703, 2000.
4) Kishikawa K, Kamouchi M, Okada Y, Inoue T, Ibayashi S, Iida M. Evaluation of diatal extracranial internal carotid artery by transoral carotid ultrasonography in patients with severe carotid stenosis. Am J Neuroradiol **23**: 924–928, 2002.
5) Adams HP Jr, Bendixen BH, Kappelle LJ, et al. TOAST investigator: classification of subtype of acute ischemic stroke. Definitions for use in a multicenter clinical trial, Trial of Org 10172 in Acute Stroke Treatment. Stroke **24**: 35–42, 1993.
6) National Institute of Neurological Disorders and Stroke. Classification of cerebrovascular disease III. Stroke **21**: 637–676, 1990.
7) Ringelstein EB, Zeumer H, Angelou D. The pathogenesis of strokes from internal carotid artery occlusion. Diagnositc and therapeutic implications. Stroke **14**: 867–875, 1983.
8) Bartels E. Carotid system in: Color-Coded Duplex Ultrasonography of the Cerebral Vessels: *Atlas and Manual.* Barteles E, Ed. Stuttgart, Schattauer, 1999: 59–112.
9) Easton JD, Sherman DG. Management of cerebral embolism of cardiac origin. Stroke **11**: 433–442, 1980.

Case Report

Cerebrovascular Diseases

Published online: February 7, 2005

Cerebrovasc Dis 2005;19:201–205
DOI: 10.1159/000083877

Cerebral Infarction Associated with Essential Thrombocythemia: An Autopsy Case Study

Jun Ogata[a], *Kiminobu Yonemura*[b], *Kazumi Kimura*[b], *Chikao Yutani*[a], *Kazuo Minematsu*[b]

[a]Department of Pathology and [b]Cerebrovascular Division, Department of Medicine, National Cardiovascular Center, Osaka, Japan

Introduction

Essential thrombocythemia (ET) is a myeloproliferative disorder with a high incidence of thrombotic complications. Cerebral ischemia is often the presenting feature of ET [1–3]. No clear correlation has been established between the absolute platelet count and the risk of thrombosis, implicating abnormal platelet function as a cause of thrombosis [1, 2]. Although postmortem pathological studies of cases with cerebral infarction associated with ET have revealed evidence of pathogenetic mechanisms, few postmortem pathological studies of ET have been reported. We report on an autopsy case of cerebral infarction associated with ET showing thrombus formation in relation to cerebral artery stenosis.

Methods of ex vivo Platelet Aggregation Test

Ex vivo platelet aggregation was measured in our hospital laboratory [4] by the method of Ieko et al. [5] based on the principle of Born and Cross [6]. With an aggregometer (Meba 1 Aggrecoder PAM 1; MC Medical, Tokyo, Japan), platelet aggregation was observed for 10 min after the addition of adenosine diphosphate (ADP) at a final concentration of 1.7 μmol/l or collagen at a final concentration of 1.7 μg/ml to platelet-rich plasma. The maximum aggregation was expressed as a percent of increase in light transmission. Absorbance of platelet-rich plasma was adjusted as 0% and of platelet-poor plasma as 100%. The normal values of the platelet aggregation in the control subjects were 44.1 ± 23.5% (mean ± SD) to ADP and 84.5 ± 8.4% to collagen, respectively [4]. The condition of the aggregation test had been rigidly followed throughout the study.

Case Report

First Admission for Transient Ischemic Attacks. A 62-year-old man was admitted to our hospital in 1983 for 3 transient episodes of speech arrest and right hemiparesis within 3 weeks. He had suffered from a gastric ulcer at the age of 42 and had had a transurethral resection of prostate hypertrophy at the age of 44. His blood pressure was 128/82 mm Hg, and physical examination and routine diagnostic examinations showed no abnormalities. In addition, no risk factor for cerebral infarction was noted. His platelet count was 332,000/μl, hemoglobin 12.6 g/dl and serum total cholesterol 149 mg/dl. Brain computed tomography (CT) and cerebral angiography showed no abnormalities. The transient ischemic attacks (TIAs) ceased after the administration of ticlopidine at 300 mg a day. Within 5 months, the dose was reduced to 200 mg. ADP-induced platelet aggregation was decreased (percent of increase in light transmission: 10, 13, 5%) while administering ticlopidine 200 or 300 mg a day, during which the examination was not performed before the antiplatelet therapy. His platelet count insidiously increased in the absence of a definable cause: 485,000/μl at the age of 65, 560,000/μl at the age of 71 and 753,000/μl at the age of 72.

Second Admission for a TIA at the Age of 74. A transient left medial longitudinal fasciculus syndrome associated with presyncopal dizziness developed 12 days after discontinuing ticlopidine on schedule for a transurethral resection of prostate hypertrophy. The platelet count was 793,000/μl. Without ticlopidine, the ADP-induced platelet aggregation was increased (89, 85%). After restarting ticlopidine 200 mg a day, cerebral ischemia did not recur, and the ADP-induced platelet aggregability was decreased (3%). Brain magnetic resonance imaging (MRI) and magnetic resonance angiography (MRA) showed no abnormalities. His platelet count remained elevated, and the count was 728,000/μl at the age of 75.

Third Admission for a Reversible Ischemic Neurological Deficit at the Age of 75. Dysarthria lasting 17 days occurred while on ticlopidine. ADP-induced platelet aggregation, which had not been examined for 15 months since the last admission, was increased (74, 85%) with ticlopidine. Brain MRI and CT showed the development of small deep infarcts which were not enhanced with contrast medium in the right pontine base and left cerebellar hemisphere. The MRA showed no abnormalities. Three weeks after the reversible ischemic neurological deficit (RIND), antiplatelet agents were changed to a daily dose of ticlopidine 100 mg and Aspirin 81 mg. This decreased collagen-induced platelet aggregation (10%), while ADP-induced platelet aggregation was not decreased (33%). Due to the onset of a RIND while on ticlopidine, ineffective ticlopidine at an ordinary dose for ADP-induced platelet aggregation and an increased platelet count up to 1,020,000/μl, ramimustine, an antitumor alkylating agent, was administered for 2 months, 5 months after the RIND to reduce the platelet count. This resulted in a decrease to 390,000/μl, and it was not long before the count reverted to the previous level. His counts were 746,000/μl at the age of 76 and 688,000/μl at the age of 77. Aspirin was withdrawn after 15 months because of epigastric pain and prolonged bleeding time, while 100 mg ticlopidine administration was continued.

Fourth Admission for Left Parietal Lobe Infarction at the Age of 77. The patient developed right hemiparesis while on ticlopidine. A brain MRI, including diffusion-weighted imaging, showed a fresh infarct of the left superior and inferior parietal lobules (measuring 5 × 4 × 3 cm; fig. 1a). Cerebral angiography performed 10 days after the onset of the infarction revealed a segmental wall irregularity with the maximum stenosis of 50% of the major branch of the left middle cerebral artery (M2; fig. 2a). There was no left M2 branch shortly distal to the wall irregularity, which was visualized on the angiogra-

Fax + 41 61 306 12 34
E-Mail karger@karger.ch
www.karger.com

Accessible online at:
www.karger.com/ced

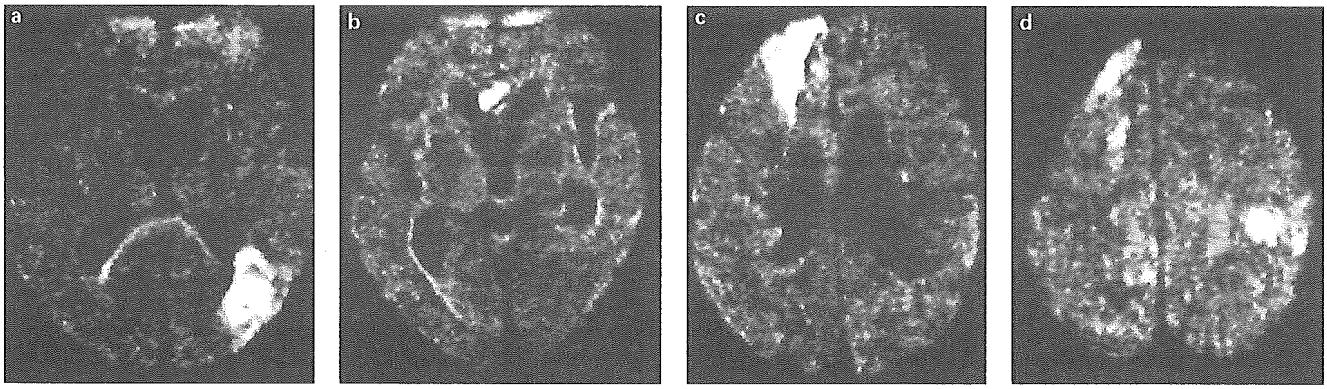

Fig. 1. a Diffusion-weighted axial MRI performed 5 days after the onset of right hemiparesis, which occurred 13 months before death, shows a hyperintensity area in the left parietal lobe. **b–d** Diffusion-weighted MRIs performed 6 days after the onset of somnolence and left hemiparesis, which occurred 20 days before death, reveal hyperintensity areas in the right frontal lobe, corpus callosum and left parietal lobe.

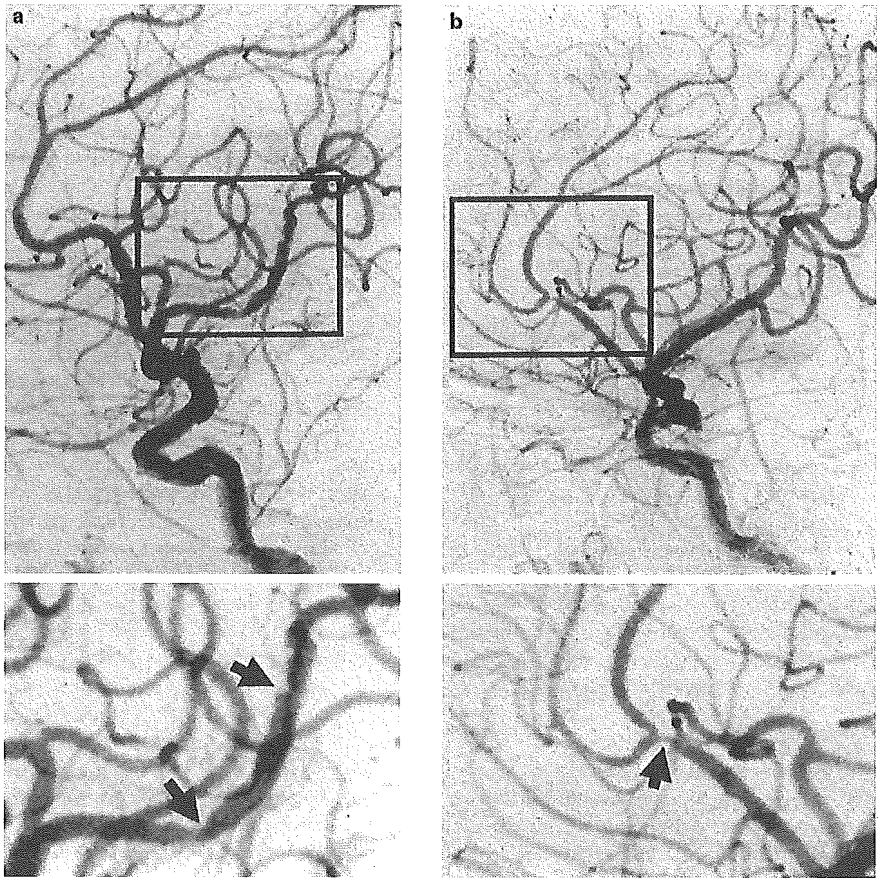

Fig. 2. Left (**a**) and right (**b**) carotid angiograms performed 10 days after the onset of right hemiparesis, which occurred 13 months before death, restrictively show stenosis of the left M2 and right A2. The enclosed areas are enlarged below for the stenosis (arrows).

phy taken at the age of 62. There was another site of 60% stenosis at the major branch of the right anterior cerebral artery (A2) just proximal to the origin of the pericallosal artery (fig. 2b). ADP-induced platelet aggregation was increased (82, 75%) on admission. Two months after the onset of the left parietal lobe infarction, plasma β-thromboglobulin was 135 ng/ml (normal range <50 ng/ml), and platelet factor 4 was 52 ng/ml (normal range <20 ng/ml) as determined by the enzyme immunoassay method. A bone marrow biopsy revealed an increase in the population of megakaryocytes. Another attempt to reduce the platelet count was made with the administration of hydroxycarbamide, an antitumor antimetabolite, but this was discontinued after 1 month because he developed pneumonia.

Fifth (Final) Admission for Left Parietal Lobe and Right Frontal Lobe Infarction at the Age of 78. The patient was admitted for somnolence and left hemiparesis while on ticlopidine 100 mg a day 13 months after the left parietal lobe infarction. He was emaciated and showed bronchopneumonia. A brain MRI showed fresh infarcts of the right frontal lobe measuring 4.5 × 4 × 3 cm and the corpus callosum, and of the left superior parietal lobule measuring 2 × 2 × 1.5 cm next to the old cystic infarct (fig. 1b–d). His platelet count was 686,000/μl on admission, and ADP-induced platelet aggregation was increased (78%) in spite of ticlopidine administration. The patient died of bronchopneumonia 20 days after the onset of the left parietal and right frontal lobe infarction.

Throughout the whole clinical course, the necessary results were obtained by repeated examinations as follows. Risk factors for cerebral infarction: other than thrombocythemia, there was no risk factor for cerebral infarction, such as hypertension, diabetes mellitus, arrhythmia, hypercholesterolemia, hyperfibrinogenemia, elevated C-reactive protein values and hematological disorders including polycythemia, anemia, abnormal prothrombin and partial thromboplastin times, presence of lupus anticoagulants and anticardiolipin antibodies, and functional deficiencies of antithrombin III and protein C.

Ex vivo platelet aggregation test: ADP-induced platelet aggregation was increased while administering no antiplatelet agent and was decreased with ticlopidine until the age of 74, while the aggregability was increased with a dose of 200 mg a day at the age of 75 and with 100 mg a day thereafter. Collagen-induced platelet aggregation was normal while taking no antiplatelet agent, and was not influenced by ticlopidine.

Echocardiography: No abnormalities.

Ultrasonography of the extracranial carotid and vertebral arteries: no carotid artery plaque and normal flow patterns.

Postmortem Pathological Examination

The lungs showed bronchopneumonia, and a healed gastric ulcer was found. The bone marrow of the lumbar vertebra revealed a moderate increase in diffusely distributed large megakaryocytes with multilobulated nuclei (cell density: 14–34/mm^2, cell diameter: 35–70 μm) and was normocellular with normal erythroid and myeloid cells. There was a tendency of such megakaryocytes to cluster in 2–4 cell groups. The fatty component of the marrow was not increased. Argentophilic fibers were not increased in Gomori's stain, and stainable iron was not found in Berlin blue stain. The spleen (60 g, body height: 162 cm, body weight: 38 kg) and liver showed no specific pathological changes. The heart was not hypertrophic (285 g, left ventricular wall thickness: 10 mm) and showed neither abnormalities of the valves nor thrombi in the chambers. The kidneys showed slight to moderate intimal fibrosis of the small arteries of the cortex, while arteriolar hyalinization was not found in the periodic acid-Schiff reaction.

Fibrous plaques and fatty streaks were scattered over the aorta. There was no complicated lesion, such as a plaque with hemorrhage, thrombosis, ulceration or dissection. The severity of atherosclerosis of the aorta was slight corresponding to grade 2 of the 7 intervals of the American Heart Association panel score [7]. There was no fibrous plaque in the extracranial cervical arteries.

Sections of the brain showed a fresh pale infarct next to the superior portion of the old cystic infarct of the left parietal lobe. There were fresh pale infarcts of the right frontal lobe and corpus callosum.

Sequential sections of the major arteries at the base of the brain showed atherosclerotic stenosis localized at and shortly proximal to the segments occluded with fresh and old thrombi, while there was no plaque rupture or intraplaque hemorrhage at the stenotic lesions. The areas of fresh and old parietal lobe infarcts were supplied by a left M2 with atherosclerotic stenotic plaques. This M2 was bifurcated 5 mm distal to the stenosis into two branches, one of which was occluded with organized thrombi at the beginning of the bifurcation and the other with fresh thrombi at the stenosis. The right A2 supplying the right frontal lobe and corpus callosum infarcts was occluded with fresh thrombi at the stenosis (fig. 3d). Atherosclerotic changes in the major arteries at the base of the brain other than the left M2 and right A2 plaques were slight. The areas involved with the infarcts of the cerebral hemispheres were the whole territories supplied by the occluded brain arteries.

The luminal diameter and the original luminal diameter surrounded by internal elastic lamina of the most stenotic portion of the artery involved with a plaque, on histological sections, were 375 and 2,050 μm (an 82% stenosis) in the left M2 and 375 and 1,625 μm (a 77% stenosis) in the right A2, respectively.

The fresh thrombi occluding the left M2 and the right A2 consisted of eosinophilic granular material with a minimum or totally absent fibrin component on phosphotungstic acid hematoxylin staining. The thrombi were infiltrated with a small number of reactive cells and showed early neovascular formation. The ultrastructure of the occlusive thrombus of the right A2 revealed aggregates of degenerating platelets with secretory granules in the cytoplasm and a few pseudopods, a small amount of fibrin, and some erythrocytes. The fresh thrombi were stained positive with a monoclonal antibody against human CD41, platelet glycoprotein IIb, 5B12 (Dako Cytomation Denmark A/S, Glostrup, Denmark; fig. 3a–d).

There were two small old deep infarcts, one measuring 4 × 2 × 2 mm in the right pontine base, and another measuring 3 × 2 × 2 mm in the white matter of the left cerebellar hemisphere. No vascular lesion responsible for the small infarcts was found. Some penetrating arteries of the basal ganglia only showed mural fibrosis. No cerebral amyloid angiopathy was noted in the sections stained with a monoclonal antibody against human β-amyloid (Dako Cytomation Denmark A/S). There was no microvascular occlusion, microinfarct or petechial hemorrhage in the brain slices other than the large and small deep infarcts. The density of the neuritic plaques in the cerebral cortex and neurofibrillary tangles in the hippocampus was sparse.

There was no thrombus elsewhere in the body.

Discussion

We described the whole clinical course and postmortem pathological findings of a case with sustained elevation of the platelet count

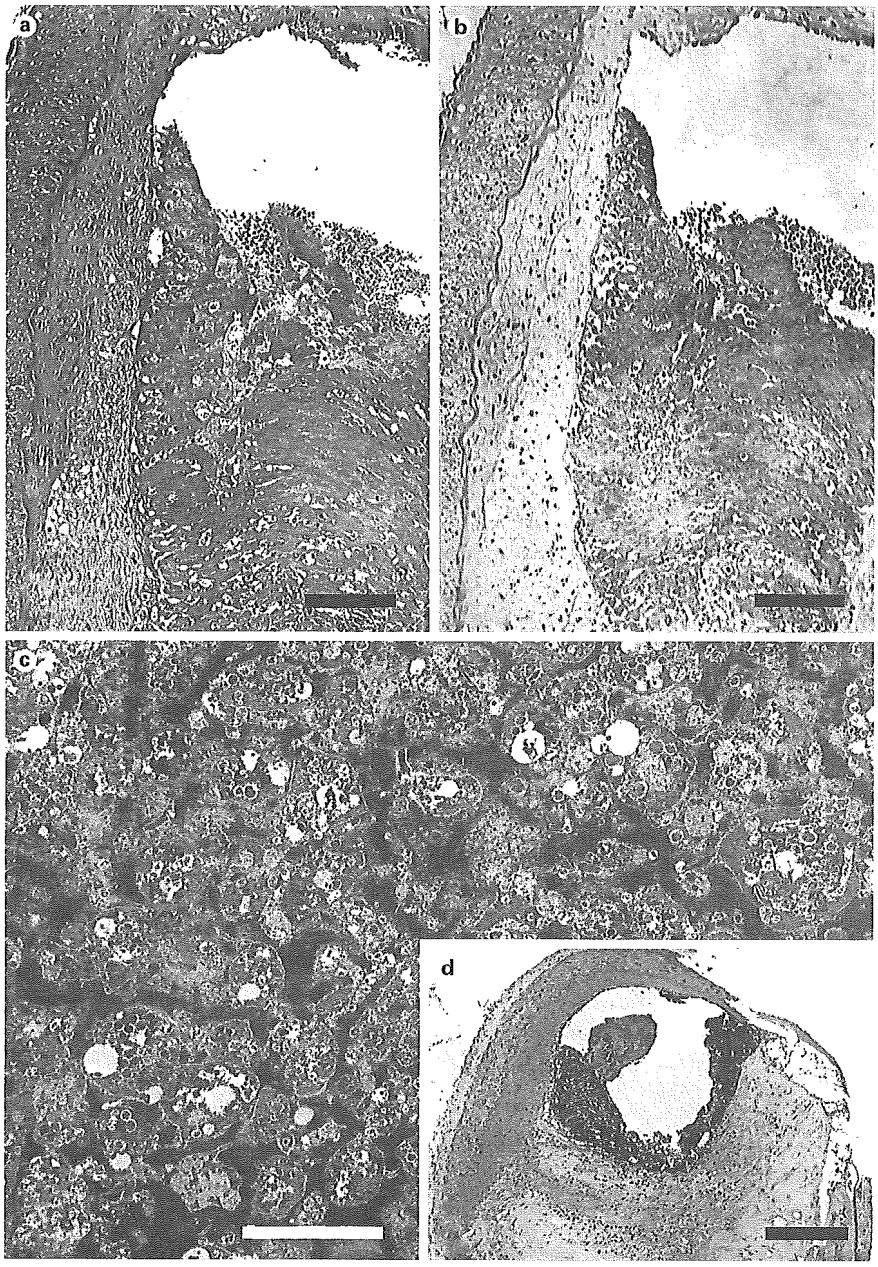

Fig. 3. **a** A section of the fresh thrombus of the left M2. The thrombus consisted of eosinophilic material infiltrated with early reactive cells. Hematoxylin and eosin. **b** A parallel section of **a** shows the thrombus stained positive for an antibody against the platelet glycoprotein. Immunostaining with an antibody against CD41. Scale bar = 200 μm. **c** Ultrastructure of the fresh thrombus of the right A2. The thrombus consisted of degenerating platelets intervened by dark strands of fibrin. Scale bar = 5 μm. **d** Section of the right A2. Atherosclerotic stenosis and fresh mural thrombus. Hematoxylin and eosin. Scale bar = 500 μm.

with values in excess of 400,000/μl for 13 years in the absence of a definable cause, such as chronic inflammation, iron deficiency, splenectomy or malignant disease. The bone marrow showed an increase in clustered large megakaryocytes [8]. A diagnosis of ET was made in this case according to the criteria of the Polycythemia Vera Study Group [9]. TIAs began to take place in this case showing no risk factors for cerebral infarction and with normal cerebral angiography. The TIAs were well controlled with ticlopidine over an extended time, while ticlopidine therapy turned out to be ineffective as far as the cerebral ischemic events were concerned with the passing of time associated with elevation of the platelet count. The mechanism of failure of ticlopidine therapy late in the clinical course is unknown. Localized atherosclerotic plaques in the major branches of the circle of Willis, which developed later, gave rise to in situ development of occlusive platelet thrombi. Artery-to-artery embolism was excluded through the postmortem pathological study.

The clinical laboratory examinations for platelet function of this case revealed increased ADP-induced platelet aggregation with normal collagen-induced platelet aggregation and increased plasma levels of in vivo secreted platelet-specific proteins.

The previous ET studies for platelet function showed impairment in platelet aggregation. ADP-, collagen- or adrenalin-induced platelet

aggregation was decreased in a high percentage of ET patients [10, 11], while they were not decreased in ET patients with thrombotic complications [12]. Adrenalin-induced platelet aggregation distinguished best between ET patients and patients with reactive thrombocytosis or healthy controls [10]. The circulating platelet aggregate [12] and spontaneous platelet aggregation values [10, 12], which are indicative of activation of platelet aggregation in vivo, were higher in ET patients. Plasma β-thromboglobulin and platelet factor 4 [11] as well as urinary excretion of the major enzymatic metabolites of thromboxane B_2 [13] were increased in ET patients. Nevertheless, similar platelet hyperaggregability has been observed in other unrelated clinical conditions, and some of the abnormalities reported in ET patients could be a consequence of ongoing subclinical thrombosis [1]. At all events, no specific platelet function abnormality to explain the propensity for thrombotic complications in ET patients has been elucidated.

Explanations as to why the authors consider that the changes in this case are different from an elderly patient with severe atherosclerosis of the cerebral arteries who did not have ET are as follows. First, ischemic cerebral events developed in a patient with no risk factors for cerebral infarction and with no abnormalities in cerebral angiography. Second, occlusive platelet thrombi developed at the uncomplicated atherosclerotic plaque with stenosis of moderate severity at 50 and 60% on angiography. Our study revealed increased ADP-induced platelet aggregation in a case with ET. Therefore, the increased platelet aggregation, the evidence of which was confirmed in ADP-induced aggregation, is considered to have played a role in the cerebral ischemia. The TIAs and thrombus formation at stenosis of moderate severity may, of course, take place in elderly patients who do not have ET, but it is not likely for elderly patients who do not have ET readily to develop these cerebral ischemic events.

We believe that the pathological platelet hyperaggregability in a case with ET exacerbated shear-induced platelet aggregation at the stenosis [14, 15] of the cerebral arteries, thereby enabling platelet thrombi to form in situ. Moreover, at two sites of the major arteries where no abnormalities were observed in the cerebral angiography 15 years before the major thrombotic event, localized atherosclerosis developed. Atherosclerosis of the circle of Willis and the major branches other than the left M2 and right A2 plaques was slight. Therefore, increased platelet aggregability and local blood flow peculiar to these sites may have been responsible for the development of the localized atheromatous plaques.

In conclusion, autopsy evidence was provided regarding thrombus formation in cerebral artery stenosis for a case of platelet hyperaggregability associated with ET, where shear-induced platelet aggregation at the stenosis could have played a role.

Acknowledgments

This study was supported in part by Research Grants for Cardiovascular Disease (15C-1) from the Ministry of Health, Labor and Welfare, Japan.

References

1 Schafer AI: Essential thrombocythemia. Prog Hemost Thromb 1991;10: 69–96.
2 Hart RG, Kanter MC: Hematologic disorders and ischemic stroke: A selective review. Stroke 1990;21:1111–1121.
3 Michiels JJ, Koudstaal PJ, Mulder AH, van Vliet HHDM: Transient neurologic and ocular manifestations in primary thrombocythemia. Neurology 1993;43:1107–1110.
4 Sakata T, Kobayashi K, Katayama Y, Takada T, Matsuyasa T: Clinical evaluation of platelet antagonists on the ex vivo inhibitory effects of platelet aggregation (Japanese with English abstract). Jpn J Clin Pathol 1991;39: 315–320.
5 Ieko M, Tarumi T, Takeda M, Naito S, Nakabayashi T, Koike T: Synthetic selective inhibitors of coagulation factor Xa strongly inhibit thrombin generation without affecting initial thrombin forming time necessary for platelet activation in hemostasis. J Thromb Haemost 2004;2:612–618.
6 Born GVR, Cross MJ: The aggregation of blood platelets. J Physiol 1963; 168:178–195.
7 McGill HC Jr, Brown BW, Gore I, McMillan GC, Patterson JC, Pollack OJ, Roberts JC Jr, Wissler RW. Grading human atherosclerosis lesions using a panel of photographs. Circulation 1968;37:455–459.
8 Burkhardt R, Bartl R, Jager K, Frisch B, Kettner G, Mahl G, Sund M: Chronic myeloproliferative disorders (CMPD). Pathol Res Pract 1984;179: 131–186.
9 Michiels JJ, Juvonen E: Proposal for revised diagnostic criteria of essential thrombocythemia and polycythemia vera by the Thorombocythemia Vera Study Group. Semin Thromb Hemost 1997;23:339–347.
10 Hehlmann R, Jahn M, Maumann B, Köpck W: Essential thrombocythemia: Clinical characteristics and course of 61 cases. Cancer 1988;61:2487–2496.
11 Bellucci S, Ignatova E, Jaillet N, Boffa MC: Platelet hyperactivation in patients with essential thrombocythemia is not associated with vascular endothelial cell damage as judged by the level of plasma thrombomodulin, protein S, PAI-1, t-PA, and vWF. Thromb Haemost 1993;70:736–742.
12 Wu KK: Platelet hyperaggregability and thrombosis in patients with thrombocythemia. Ann Intern Med 1978;88:7–11.
13 Rocca B, Ciabattoni G, Tartaglione R, Cortelazzo S, Barbui T, Patrono C, Landolfi R: Increased thromboxane biosynthesis in essential thrombocythemia. Thromb Haemost 1995;74:1225–1230.
14 Uchiyama S, Yamasaki M, Maruyama S, Handa M, Ikeda Y, Fukuyama M, Itagaki I: Shear-induced platelet aggregation in cerebral ischemia. Stroke 1994;25:1547–1551.
15 Konstantopoulos K, Grotta JC, Sills C, Wu KK, Hellums JD: Shear-induced platelet aggregation in normal subjects and stroke patients. Thromb Haemost 1995;74:1329–1334.

Jun Ogata, MD
Hirakata Ryoikuen, Tsudahigashi-machi 2-1-1
Hirakata, Osaka 573-0122 (Japan)
Tel. +81 72 858 0373, Fax +81 72 858 9521
E-Mail jogata@hirakataryoiku-med.or.jp

Atherosclerosis Found on Carotid Ultrasonography Is Associated With Atherosclerosis on Coronary Intravascular Ultrasonography

Toshiyasu Ogata, MD, Masahiro Yasaka, MD, Masakazu Yamagishi, MD, Osamu Seguchi, MD, Kazuyuki Nagatsuka, MD, Kazuo Minematsu, MD

Objective. Little has been reported on the relationship between left main coronary artery atherosclerosis and carotid ultrasonographic results. We evaluated the association between carotid and coronary atherosclerosis assessed by coronary intravascular ultrasonography (IVUS) in 45 patients. ***Methods.*** We counted the number of plaques with intima-media thickness (IMT) greater than or equal to 1.1 mm and calculated a plaque score by summing all plaque thicknesses. With the use of IVUS, the percent plaque area was calculated at the proximal, middle, and distal sites of the left main coronary artery. The maximum percent plaque area and mean percent plaque area of the 3 sites were also calculated. Relationships among the degree of left main coronary artery atherosclerosis and carotid atherosclerosis and vascular risk factors were evaluated. ***Results.*** The mean percent plaque area and maximum percent plaque area were increased in men and in patients with hypertension compared with women and those without hypertension ($P < .1$). Both the average of the maximum common carotid IMT and plaque number were correlated with both the mean percent plaque area and maximum percent plaque area ($P < .05$). Men, the presence of hypertension, and the average of the maximum common carotid IMT were correlated with both the mean percent plaque area and maximum percent plaque area by multiple linear regression analysis ($P < .05$). ***Conclusions.*** The average of the maximum common carotid IMT was significantly correlated with left main coronary artery atherosclerosis evaluated by IVUS. ***Key words:*** atherosclerosis; carotid arteries; coronary disease; ultrasonography.

Abbreviations
CAD, coronary artery disease; IMT, intima-media thickness; IVUS, intravascular ultrasonography

Received September 30, 2004, from the Cerebrovascular (T.O., M.Y.as., K.N., K.M.) and Cardiovascular (M.Yam., O.S.) Divisions, Department of Medicine, National Cardiovascular Center, Osaka, Japan. Revision requested October 18, 2004. Revised manuscript accepted for publication November 17, 2004.

This study was partially supported by a research grant from the Ministry of Health, Labor, and Welfare, Japan (15A-1).

Address correspondence and reprint requests to Toshiyasu Ogata, MD, Department of Medicine and Clinical Science, Kyushu University, Maidashi 3-1-1, Higashi-ku, Fukuoka 812-8582, Japan.
E-mail: togata@intmed2.med.kyushu-u.ac.jp

Several studies have identified a relationship between the presence of carotid artery disease and coronary artery disease (CAD). An autopsy study showed a strong correlation between the extent of carotid and coronary atherosclerosis.[1,2] Both arterial beds share risk factors that contribute to the progression of atherosclerosis.[3,4] Ultrasonography is used to assess the presence and extent of atherosclerosis in the carotid and coronary arteries. The carotid intima-media thickness (IMT) has been shown to be a good index of the presence and extent of CAD.[5-8] Also, there is evidence of a strong relationship between the presence of carotid plaques and coronary lesions.[9-12]

Patients with severe left main CAD are known to have a poor long-term prognosis.[13–15] Although coronary angiography is considered the criterion standard for the diagnosis of left main CAD, the degree of atherosclerosis is often underestimated by this method. In contrast, intravascular ultrasonography (IVUS) has been shown to be more accurate and sensitive than coronary angiography in identifying left main coronary artery lesions.[16] Although increased IMT on carotid ultrasonography has been used as a noninvasive marker for CAD, there have been few reports assessing the relationship between left main coronary artery atherosclerosis and carotid ultrasonographic results directly.

The aim of this study was to determine whether atherosclerosis detected in the carotid arteries by carotid ultrasonography was related to the extent of left main coronary artery atherosclerosis evaluated by IVUS.

Materials and Methods

Between November 1, 2000, and December 31, 2002, carotid ultrasonography was performed on 45 Japanese patients (40 men and 5 women; mean age ± SD, 60.8 ± 10.7 years; median age, 62 years) with CAD who also underwent coronary angiography. This study was approved by the Ethics Committee of our hospital. We obtained informed consent about coronary angiography and IVUS from all patients or their families. Coronary angiography was performed by a standard technique to assess the number of involved vessels.

If CAD of more than 1 vessel was detected on coronary angiography, IVUS studies were performed with a single-element 30-MHz, 2.9F or 3.2F intracoronary ultrasonographic catheter (Hewlett-Packard Company, Palo Alto, CA) (Figure 1). The IVUS transducer (30-40 MHz, 1800 rpm) was carefully advanced to the distal site of the patient's left main coronary artery, and the transducer was automatically pulled back (0.5 or 1.0 mm/s) by a motorized pullback device (Cardiovascular Imaging Systems/Boston Scientific, Natick, MA). Special care was taken to visualize the vessel lumen circularly rather than elliptically. If the lumen appeared elliptical, the transducer was repositioned as centrally as possible in the vessel. All images were recorded on super VHS videotape for subsequent analysis.

Ultrasonographic measurements were performed with an offline computer. The vessel lumen area was determined by tracing the leading edge of the intima. The external elastic membrane area was determined by tracing the leading edge of the second bright echo.[17] The percent plaque area was calculated as {(external elastic membrane area − lumen area)/external elastic membrane area} × 100. It was measured at proximal, middle, and distal sites. The maximum percent plaque area and mean percent plaque area of the 3 measurements were used in this study. Calcification of the left main coronary artery was considered present if there was high echo density with acoustic shadowing of the plaque.[12]

Carotid ultrasonography was carried out by experienced clinicians (T.O. and M.Yas.) using an Ultramark 9 HDI unit (Philips Medical Systems, Bothell, WA) with a linear array pulsed wave transducer operating at 5.0 to 10.0 MHz. Neither of them knew about the results of the IVUS study. The pulse repetition frequency was primarily 5000 Hz, and the low-pass filter was 50 Hz. Imaging was performed while the patients were lying in a supine position with their head turned away from the side being scanned and neck extended. The origin of the internal carotid artery was examined in longitudinal and transverse planes.

The IMT was evaluated by 2 calipers on the frozen frame of a suitable longitudinal image as the distance between the luminal-intimal interface and the medial-adventitial interface of the artery. We measured the maximum IMT of each

Figure 1. Representative IVUS image of the left main coronary artery.